Journal of Diabetes and Its Complications 38 (2024) 108722

Contents lists available at ScienceDirect

Journal of Diabetes and Its Complications

journal homepage: www.elsevier.com/locate/jdiacomp

Research paper

Analysis of the therapeutic potential of miR-124 and miR-16 in non-alcoholic fatty liver disease

Ali Mahmoudi [a], Amin Jalili [a,*], Seyed Hamid Aghaee-Bakhtiari [b,a], Reza Kazemi Oskuee [c,d], Alexandra E. Butler [e], Manfredi Rizzo [f,g], Amirhossein Sahebkar [c,h,**]

[a] Department of Medical Biotechnology and Nanotechnology, Faculty of Medicine, Mashhad University of Medical Sciences, Mashhad, Iran
[b] Bioinformatics Research Center, Mashhad University of Medical Sciences, Mashhad, Iran
[c] Applied Biomedical Research Center, Mashhad University of Medical Sciences, Mashhad, Iran
[d] Targeted Drug Delivery Research Center, Institute of Pharmaceutical Technology, Mashhad University of Medical Sciences, Mashhad, Iran
[e] Research Department, Royal College of Surgeons in Ireland, Bahrain, Adliya, Bahrain
[f] School of Medicine, Department of Health Promotion, Mother and Child Care, Internal Medicine and Medical Specialties (Promise), University of Palermo, Italy
[g] Department of Biochemistry, Mohamed Bin Rashid University, Dubai, United Arab Emirates
[h] Biotechnology Research Center, Pharmaceutical Technology Institute, Mashhad University of Medical Sciences, Mashhad, Iran

ARTICLE INFO

Keywords:
NAFLD
Real-time PCR
miR-124
miR-16
Transfection

ABSTRACT

Backgrounds: Non-alcoholic fatty liver disease (NAFLD) is a common condition affecting >25 % of the population worldwide. This disorder ranges in severity from simple steatosis (fat accumulation) to severe steatohepatitis (inflammation), fibrosis and, at its end-stage, liver cancer. A number of studies have identified overexpression of several key genes that are critical in the initiation and progression of NAFLD. MiRNAs are potential therapeutic agents that can regulate several genes simultaneously. Therefore, we transfected cell lines with two key miRNAs involved in targeting NAFLD-related genes.

Methods: The suppression effects of the investigated miRNAs (miR-124 and miR-16) and genes (TNF, TLR4, SCD, FASN, SREBF2, and TGFβ-1) from our previous study were investigated by real-time PCR in Huh7 and HepG2 cells treated with oleic acid. Oil red O staining and the 3-(4,5-dimethylthiazol-2-yl)-2,5-diphenyl-2H-tetrazolium bromide (MTT) assay were utilized to assess cell lipid accumulation and cytotoxic effects of the miRNAs, respectively. The pro-oxidant-antioxidant balance (PAB) assay was undertaken for miR-16 and miR-124 after cell transfection.

Results: Following transfection of miRNAs into HepG2, oil red O staining showed miR-124 and miR-16 reduced oleic acid-induced lipid accumulation by 35.2 % and 28.6 % respectively ($p < 0.05$). In Huh7, miR-124 and miR-16 reduced accumulation by 23.5 % and 31.3 % respectively ($p < 0.05$) but without impacting anti-oxidant activity. Real-time PCR in HepG2 revealed miR-124 decreased expression of TNF by 0.13-fold, TLR4 by 0.12-fold and SREBF2 by 0.127-fold ($p < 0.05$). miR-16 decreased TLR4 by 0.66-fold and FASN by 0.3-fold ($p < 0.05$). In Huh7, miR-124 decreased TNF by 0.12-fold and FASN by 0.09-fold ($p < 0.05$). miR-16 decreased SCD by 0.28-fold and FASN by 0.64-fold ($p < 0.05$). MTT assays showed, in HepG2, viability was decreased 24.7 % by miR-124 and decreased 33 % by miR-16 at 72 h ($p < 0.05$). In Huh7, miR-124 decreased viability 42 % at 48 h and 29.33 % at 72 h ($p < 0.05$), while miR-16 decreased viability by 32.3 % ($p < 0.05$).

Conclusion: These results demonstrate the ability of miR-124 and miR-16 to significantly reduce lipid accumulation and expression of key pathogenic genes associated with NAFLD through direct targeting. Though this requires further *in vivo* investigation.

* Correspondence to: A. Jalili, Department of Medical Biotechnology and Nanotechnology, Faculty of Medicine, Mashhad University of Medical Sciences, Mashhad, Iran
** Correspondence to: A. Sahebkar, Applied Biomedical Research Center, Mashhad University of Medical Sciences, Mashhad, Iran.
E-mail addresses: jalilia@mums.ac.ir (A. Jalili), amir_saheb2000@yahoo.com (A. Sahebkar).

https://doi.org/10.1016/j.jdiacomp.2024.108722
Received 9 October 2023; Received in revised form 28 February 2024; Accepted 9 March 2024
Available online 12 March 2024

1. Introduction

Non-alcoholic fatty liver disease (NAFLD) is a common condition that affects >25 % of the population worldwide.[1] This progressive disorder ranges in severity from simple steatosis to severe steatohepatitis (NASH) and, with the advanced stages of fibrosis, can potentially progress to liver cancer.[2] A high proportion (between 35 and 50 %) of liver cancer occurs in patients with NASH.[3,4] Compared to hepatic tumors with other etiologies, these NASH-related tumors are often larger in size and less responsive to therapy.[5] The major underlying cause of NAFLD is excessive fat consumption which causes the accumulation of lipids in the liver.[6] NASH is at the severe end of the NAFLD spectrum and is characterized by inflammation.[2,6,7] Cirrhosis and liver cancer are known to be provoked by the activation of a cascade of pro-fibrogenic and pro-inflammatory cytokines as well as ongoing liver injury with the development of fibrosis.[6] Activation of hepatic stellate cells, insulin resistance, oxidative stress, mitochondrial dysfunction, aberrant release of cytokines and adipokines, obesity and lack of exercise have all been linked to the etiology and progression of NAFLD.[8,9] Although the pathophysiology of NAFLD is well defined, work to identify therapeutic targets and advances in drug research is still ongoing, and no definitive treatments are yet available for this disorder. Many genes have been reported as having a role in the pathogenesis and progression of NAFLD, such as genes known to be involved in hepatic lipid metabolism and inflammation and fibrotic pathways.[10–14] A number of studies have identified defects in the function or overexpression of genes and proteins as critical factors in the initiation and progression of NAFLD.[15,16] There is a clear need to develop multifaceted therapies that target the risk factors associated with these illnesses in order to go beyond the constraints of traditional medications.[17–19] Dysregulation or dysfunction of specific genes and pathways might lead to the initiation and progression of NAFLD and these could represent important therapeutic targets.[11–13,20,21]

In our previous bioinformatics and *in vitro* research, we reported that certain genes, specifically Tumor Necrosis Factor (TNF), Toll-Like Receptor 4 (TLR4), Stearoyl-CoA Desaturase (SCD), Fatty acid synthase (FASN), Sterol Regulatory Element Binding Transcription Factor 2 (SREBF2) and transforming growth factor beta-1 (TGFβ-1), were overexpressed in *in vitro* models of NAFLD and are also implicated in diverse stages of NAFLD including steatosis, inflammation and fibrosis.[22]

Nucleic acid-based medicines have recently undergone significant development and have shown tremendous potential as a therapeutic platform in treating a variety of disorders, some of which have already received FDA (US Food and Drug Administration) approval.[19,23]

Published studies have confirmed the effectiveness of nucleic acid-based therapeutics in the management of NAFLD. MicroRNAs are small (19–25 nucleotides) non-coding RNAs that could offer great potential as therapeutic agents in the cure of diseases such as NAFLD.[14,24] MiRNAs act as gene silencers through 3′ UTR gene binding and have several benefits such as multiple targeting and low cost in comparison to other nucleic acid-based treatments, making them excellent therapeutic candidates.[25] Approximately 2200 miRNA genes exist in the mammalian genome, and they are known to influence important cellular processes including development, growth, differentiation and metabolism. Approximately one-third of the human genome is thought to be controlled by miRNAs.[26] Available evidence confirms the role of miRNAs in regulating important genes related to hepatic steatosis and steatohepatitis.[24,27] Regulating the most important of these genes by miRNAs represents a novel approach for treating disorders such as NAFLD. In our previous *in-silico* study, we indicated miR-124 and miR-16 in particular have been shown to impact several processes central to NAFLD development, such as lipid homeostasis, autophagy, oxidative stress response, cytokine production involved in immune response, and modulation of inflammatory responses.[22] Additionally, both miRNAs inhibit TLR4 signaling and directly target genes modulating lipid metabolism and fibrosis.[28–31] Prior studies identified alternation of expression of miR-124 and miR-16 in NAFLD animal models.[32,33] Due to their roles modulating innate immune reaction, metabolic dysfunction and cross-talk between inflammatory cascades, we hypothesize miR-124 and miR-16 may hold therapeutic potential for treating NAFLD through coordinated modulation of multiple susceptibility pathways. Subsequently, we transfected two key miRNAs (miR-124 and miR-16) identified in our previous study that are known to target NAFLD-related genes including TNF, TLR4, SCD, FASN, SREBF2 and TGFβ-1.[22]

2. Materials and methods

2.1. Cell culture

Human hepatocyte cell lines (HepG2 and Huh7) were used to investigate the effect of miRNAs on the expression of target genes. We obtained cell lines from the Cell Bank of the Pasteur Institute of Iran (Tehran). Cells were maintained in RPMI-1640 medium with 10 % FBS and 1 % antibiotics (penicillin-streptomycin) in a 5 % CO_2 humidified incubator at 37 °C.

2.2. Plasmid extraction

MiR-16 and miR-124 were constructed in the form of pLenti-III-16-GFP and pLenti-III-124-GFP expression vectors which were purchased from the Stem Cell Technology Research Center vector bank (STRC, Tehran, Iran). Further, pLenti-III-GFP without miRNA was considered as a control. The *Escherichia coli Stbl4* containing the plasmids was cultured in Lysogeny broth (LB) medium with 25 μg/mL kanamycin and the DNA plasmid was refined according to Qiagen EndoFree Plasmid Maxi Kit (Qiagen, Hilden, Germany) guidelines.

2.3. NAFLD in vitro model and transfection

Huh7 and HepG2 cells were cultured in 24-well culture plates with 3 × 10^4 cells/well and 1.2 × 10^5 cells/well, respectively. pLenti-III-DNA-GFP vectors were transfected into the Huh7 and HepG2 cells with the PolyFect Transfection Reagent (Qiagen, Hilden, Germany) according to manufacturer's guidelines. To establish a fatty hepatotoxicity *in vitro* model, the cells were treated with 0.5 mM oleic acid for 36 h and the medium then replaced with fresh medium.[22] Transfection efficiency after 24 and 36 h was evaluated by fluorescent microscopy. After 36 h transfection, based on the frequency of GFP expression under fluorescent microscopy, and 12 h treating with oleic acid (0.05 mM) the cells the cells were harvested for RNA Extraction and Quantitative RT-PCR.

2.4. Oil red O staining

After 36 h transfection and 12 h treatment with oleic acid, cells were stained with oil red O. Firstly, the cells were washed with PBS buffer, incubated with formalin 10 % for 1 h, washed two times with distilled water and treated with isopropanol 60 % for five minutes. Next, cells were dried at room temperature and incubated with oil red O (Bioidea, Iran) solution for 10 min. Finally, cells were washed in sterile water four times to remove the excess dye and observed with a light microscope (magnification, 40×). To measure absorbance, stained lipid droplets were extracted by incubating for 10 min with isopropanol 100 %, and the absorbance read at 500 nm.

2.5. MiRNAs binding evaluation via computational tools against gene targets

To evaluate the binding between miRNAs (miR-16-5p and miR-124-3p) and their target genes, the sequences of miRNAs were obtained from the miRBase database, while the target gene sequences were retrieved from the NCBI Nucleotide database. The untranslated regions (UTRs) of the target genes were extracted. Using RNAhybrid 2.2 software

(Bielefeld BioInformatics Service, Bielefeld University), the miRNAs were hybridized against the UTR regions of the target genes.[34] The minimal free energy (mfe) values representing the binding energies were calculated for each miRNA-gene pair.

2.6. RNA extraction and quantitative RT-PCR

mRNA and miRNA extraction was accomplished using an RNX-Plus RNA extraction kit (SinaClon, Iran).[35,36] HepG2 and Huh7 cells (2–3 $\times 10^6$ cells) treated with 0.5 mM oleic acid and transfected with pLenti-III-16-GFP and pLenti-III-124-GFP were collected using RNX-Plus and extraction was performed according to manufacturer's instructions. The purity and quality of the extracted RNA was examined by BioPhotometer (Eppendorf, Germany). For further investigation, complementary DNA (cDNA) synthesizing RNA samples were stored at −80 °C. The cDNA synthesis from total extracted RNA was accomplished with reverse transcriptase using a cDNA Synthesis Kit (Pars Tous, Iran). Oligo dT primers for gene and designed stem-loop primers for miRNA were used for transcription of RNA to cDNA (Table 1). Real-time PCR was performed with 2× SYBR Green Real-Time PCR (Pars Tous, Iran) using the Roche LightCycler® 96 System. The forward and reverse primers for the selected genes were designed with AllelID (version 6) (Table 2) and RT-PCR was performed in triplicate. The mRNA and miRNA were normalized with GAPDH and SNORD 47 (U47) reference genes and relative expression levels were calculated by the $2^{-\Delta\Delta CT}$ technique.[37]

2.7. MTT assay

Huh7 and HepG2 cells were seeded with 4 $\times 10^3$ cells/well in 96-well culture plates, and incubated in 5 % CO_2 at 37 °C. After reaching 80 % confluency, cells were treated with 0.5 mM oleic acid and then transfected with miR-16, miR-124 and empty vector; they were then incubated for 24, 48, and 72 h. Untreated cells were considered as a control. Cells were incubated with 5 mg/mL thiazolyl blue tetrazolium bromide (MTT) solution for 3 h, after which the incubation medium was removed. Formazan crystals were dissolved in 100 μL dimethyl sulfoxide and, after rocking for 10 min, MTT reduction was quantified by measuring the absorbance value of each well with a microplate reader (BioTek, Richmond, USA) at 570 nm and 630 nm as the reference wavelength.

2.8. Pro-oxidant antioxidant balance (PAB) assay

To assess whether miR16 or miR-124 could recover the antioxidant status, an exploration of oxidant/antioxidant parameters was undertaken as detailed previously.[38] PAB (Pro-Oxidant Antioxidant Balance) was evaluated to assess the total oxidants and antioxidants in a single measurement simultaneously,[39] by oxidation of the chromogen 3,3′,5,5′-tetramethylbenzidine (TMB) to a colorless substance. In brief, the standard solution was primed in 10 mM sodium hydroxide by mixing varying amounts (0–100 %) of 250 μM hydrogen peroxide with 3 mM uric acid. This solution was dissolved in tetramethylbenzidine (TMB) (60 mg) powder and dimethyl sulphoxide (DMSO) (10 mL). To make TMB+, TMB (400 μL) was dissolved in DMSO and then mixed with M acetate buffer with pH = 4.5. Finally, peroxidase enzyme solution (25 U) was mixed with TMB+. The optical density (OD) was read for the reference at 570 or 620 nm wavelength and the sample's wavelength at 450 nm. PAB assay values were reported as arbitrary Hamidi-Koliakos (HK) units centered on the hydrogen peroxide percentage that was assessed in the standard solution.

2.9. Statistical analysis

GraphPad Prism version 9 software (GraphPad Software, LLC, Boston, USA) was used for one-way analysis of variance (ANOVA) of MTT, PAB and Oil red O staining assay. The results are presented as Mean Difference ± SE of Difference in the text and Mean ± SEM in the charts with three replicates. Mean comparison between groups was performed with Dunnett's multiple comparisons test. Rest 2009 software (QIAGEN, Technical University Munich) and was used for analyzing the real-time data (Fold change). Significant differences were reported as $^*P < 0.05$, $^{**}P < 0.01$, $^{***}P < 0.001$.

3. Results

3.1. Overexpression of miR-16 and miR-124

The pLenti-III-DNA-GFP vectors encoding miR-124, miR-16 or empty control were transfected into Huh7 and HepG2 cells using PolyFect reagent. Transfection efficiency at 24 and 36 h post-transfection was quantified by fluorescent microscopy based on GFP expression from the plasmids (Fig. 1). At 24 h, GFP fluorescence intensity was low for all groups. However, by 36 h a marked increase in GFP signal was observed for miR-124 and miR-16 transfected cells. In contrast, cells transfected with vectors alone without PolyFect did not exhibit any detectable GFP fluorescence. Based on these quantification findings, 36 h post-transfection was chosen as the optimal timepoint with sufficient overexpression of the miRNAs achieved. This timepoint was then used to induce the NAFLD model by treating cells with 0.5 mM oleic acid for 12 h prior to subsequent experiments, to ensure high miRNA levels were present during the lipotoxic insult. The outcome of selecting 36 h is that it provided consistently high transfection rates and miRNA expression to study the effects on NAFLD-related gene regulation.

3.2. Oil red O staining results

After 36 h of transfection, Huh7 and HepG2 cells were treated with 0.5 mM oleic acid for 12 h to induce lipid accumulation mimicking steatosis. Oil Red O staining was performed to visualize intracellular lipid droplets (Fig. 2A). Absorbance was then quantified spectrophotometrically at 500 nm to objectively measure total lipid content (Fig. 2B).

Absorbance values directly correlate to lipid quantity, with higher absorbance indicating greater lipid accumulation. One-way ANOVA with Tukey's multiple comparisons tests were used to determine statistical significance of differences in absorbance between groups.

In both cell lines, oleic acid treatment significantly increased lipid accumulation in empty vector control cells compared to untreated controls, as evidenced by elevated absorbance (HepG2 mean difference ± SEM: −1.83 ± 0.24, $p = 0.034$; Huh7 mean difference ± SEM: −1.59 ± 0.009, $p < 0.001$).

However, miR-124 and miR-16 overexpression mitigated this effect. Absorbance was significantly lower in miR-124 and miR-16 transfected cells *versus* empty vector, demonstrating reduced lipid content. In HepG2, miR-124 reduced absorbance by 1.48-fold ($p = 0.04$) and miR-

Table 1
The sequences of primers used for cDNA synthesis.

Gene name	Primer sequences (5′-3′)
hsa-miR-124-3p	Stem-loop primer: GTCGTATCCAGAGCAGGGTCCGAGGTATTCGCACTGGATACGACTTGGCA
hsa-miR-16-5p	Stem-loop primer: GTCGTATCCAGAGCAGGGTCCGAGGTATTCGCACTGGATACGACCGCCAA
SNORD 47	Stem-loop primer: GGAACGCTTCACGAATTTGC
Oligo dT (18)	TTTTTTTTTTTTTTTTTT

Table 2
The sequences of primers used for the qRT-PCR reaction.

Gene name	Forward primers	Reverse primers
hTLR4	TGGAAGTTGAACGAATGGAATGTG	ACCAGAACTGCTACAACAGATACT
hTGFβ-1	CCCACAACGAAATCTATGAC	AGGTATCGCCAGGAATTG
hSCD	GTGATGTTCCAGAGGAGGTACTA	TGGCATTAAGCACCACAGCA
hSREBF2	TTGTCGGGTGTCATGGGC	ACAAATTGCAGCATCTCGTCG
hTNF	TGGAAAGGACACCATGAGCA	CGAGAAGATGATCTGACTGCC
hFASN	GCAAGCTGAAGGACCTGTCT	AATCTGGGTTGATGCCTCCG
hGAPDH	CTCTGACTTCAACAGCGAC	CGTTGTCATACCAGGAAATGAG
hsa-miR-124-3p	CTAAGGCACGAGGTGAA	GAGCAGGGTCCGAGGT
hsa-miR-16-5p	GCCTAGCAGCACGTAAATA	GAGCAGGGTCCGAGGT
SNORD 47	CGCTTCGGCAGCACATATACTA	GGAACGCTTCACGAATTTGC

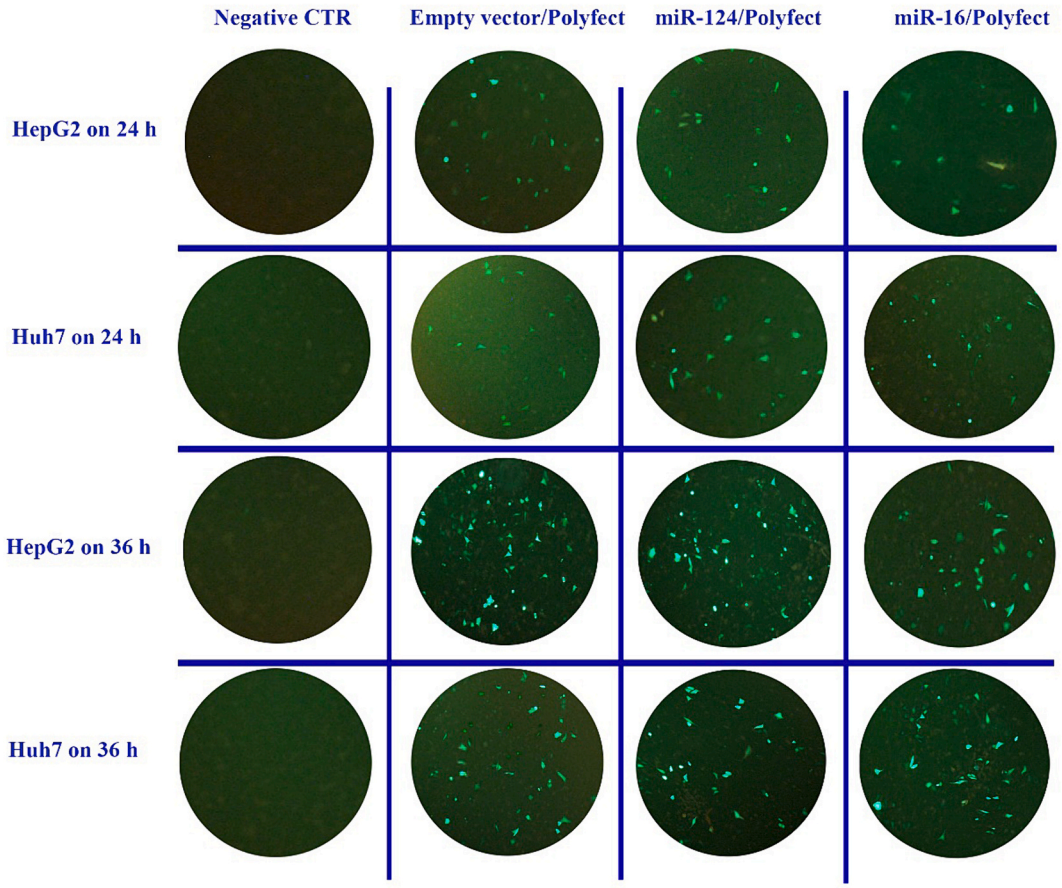

Fig. 1. Assessment of transfection efficiency in Huh7 and HepG2 cells transfected with pLenti-III-16-GFP, pLenti-III-124-GFP or empty pLenti-III-GFP vector (control) at 24 and 36 h post-transfection using PolyFect Transfection Reagent. The negative control (CTR) contains the plasmid DNA alone without Polyfect. Transfection efficiency was evaluated by fluorescence microscopy based on GFP expression from the transfected plasmids. Strong GFP fluorescence was observed at 36 h post-transfection for both miR-16 and miR-124 plasmids compared to the empty vector control, indicating high levels of overexpression had been achieved.

16 by 1.38-fold ($p = 0.048$) *versus* empty vector. Similarly, in Huh7 miR-124 lowered absorbance 1.167-fold ($p = 0.002$) and miR-16 by 1.47-fold ($p = 0.011$).

3.3. MiR-124 and miR-16 binding evaluation against gene targets

The binding evaluation (mfe: minimal free energy) between miRNAs (miR-16-5p and miR124-3p) and their target genes (TNF, TLR4, SCD, FASN, SREBF2, and TGFβ-1) was achieved using RNAhybrid 2.2 as in

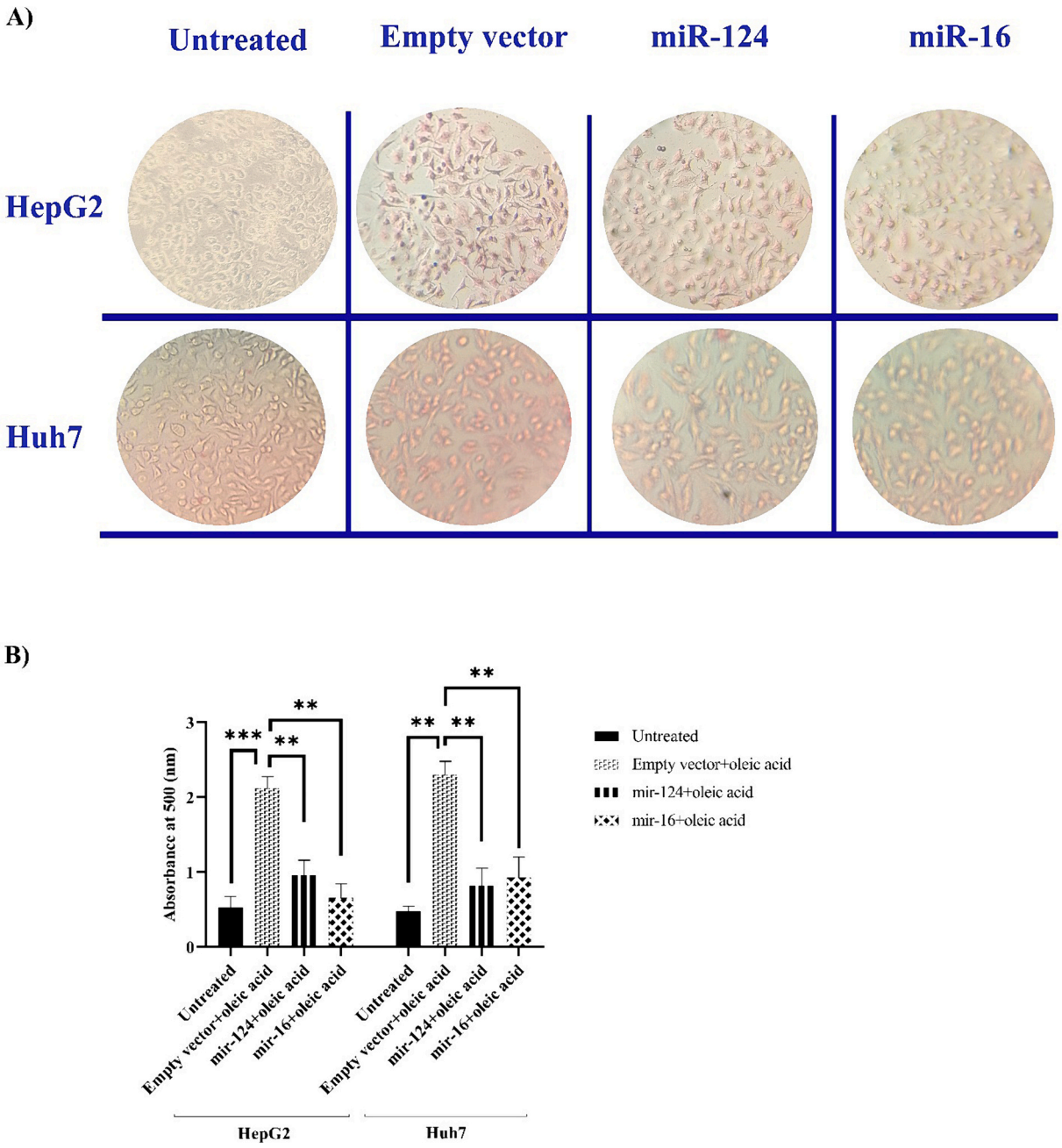

Fig. 2. Effect of miR-124 and miR-16 overexpression on oleic acid-induced lipid accumulation in Huh7 and HepG2 cells. Following 36 h of transfection with pLenti-III-16-GFP, pLenti-III-124-GFP or empty vector, the cells were treated with 0.5 mM oleic acid for 12 h to induce steatosis. (A) Lipid droplet accumulation was visualized by Oil Red O staining and light microscopy at 40× magnification. Red-stained lipid droplets are clearly visible in the empty vector control and oleic acid treated cells, while fewer droplets are seen in miR-124 and miR-16 transfected cells. (B) Oil Red O absorbance was quantified spectrophotometrically at 500 nm to objectively measure total lipid content. Absorbance was significantly higher in empty vector control cells compared to untreated control, confirming oleic acid induced steatosis. The control group lacking any oleic acid treatment served to establish baseline lipid levels.

method mentioned. The result of the hybridization of the miRNAs and gene targets demonstrated that these specific miRNAs (miR-16-4p and miR-124-3p) have a particular affinity for these target genes with most having binding energies of <20 kcal/mol (Table 3).

3.4. The result of RT-PCR evaluation

Using real-time PCR, we confirmed that the expression of miR-16 and miR-124 was upregulated in HepG2 and Huh7 cells after 36 h transfection. We found the expression of miR-16 and miR-124 were increased with a 6.5 ($P = 0.03$) and 4.37-fold change ($P < 0.001$) in HepG2 cells, respectively. Likewise, in Huh7 cells, the level of expression of miR-16 and miR-124 were upregulated, with a 5.9 ($P = 0.04$) and by 5.6-fold change ($P < 0.001$), respectively (Fig. 3-A).

3.4.1. Influence of miR-124 transfection on the target genes

Following transfection into Huh7 and HepG2 cells, Oil Red O staining showed miR-124 reduced oleic acid-induced lipid accumulation by 23.5–35.2 % and miR-16 by 28.6–31.3 % respectively compared to empty vector control. To confirm the *in vitro* effect of miR-124-3p on the level of expression of TNF, SCD, TLR4, FASN, TGFβ-1, and SREBF2 after transfection in Huh7 and HepG2 cell lines, the expression level of target

Table 3
The 2D structure of miRNAs binding with gene targets together with their minimal free energy. The red strands represent the gene targets and the green strands represent the miRNAs.

2D structure of miR16 and miR124 interaction with gene targets	miRNA and gene interaction	mfe (kcal/mol)
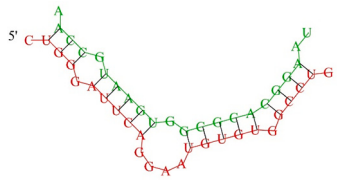	hsa-miR-124-3p: TNF	−26.4
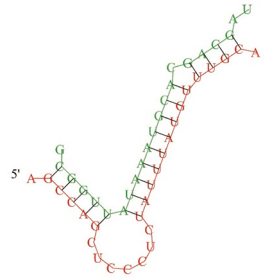	hsa-miR-16-5p: TNF	−22.7
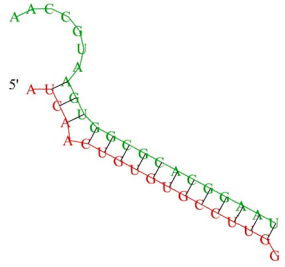	hsa-miR-124-3p: TLR4	−27.2
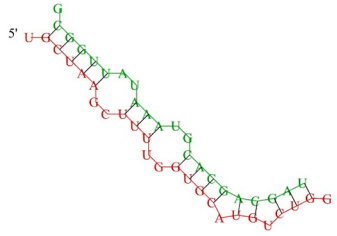	hsa-miR-16-5p: TLR4	−25.1
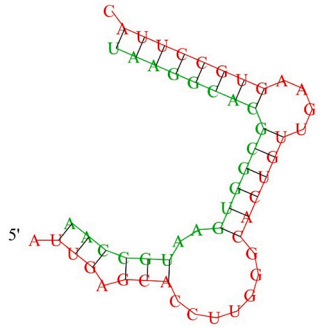	has-miR-124-3p: TGFβ-1	−27.3

Table 3 (*continued*)

2D structure of miR16 and miR124 interaction with gene targets	miRNA and gene interaction	mfe (kcal/mol)
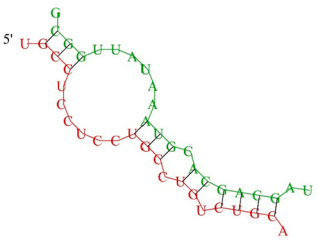	has-miR-16-5p: TGFβ-1	−19.3
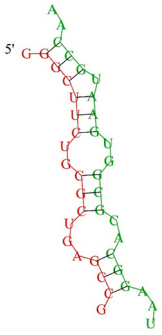	has-miR-124-3p: SREBF2	−26.5
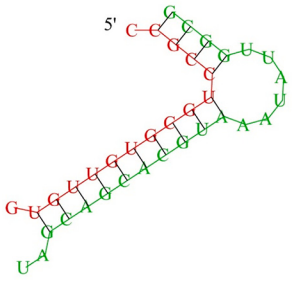	has-miR-16-5p: SREBF2	−23.9
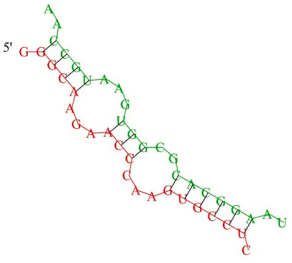	has-miR-124-3p: SCD	−26.2
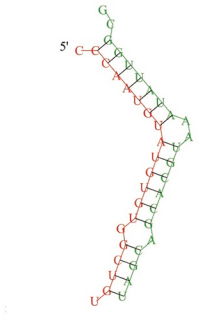	has-miR-16-5p: SCD	−23.3

(*continued on next page*)

genes was evaluated by q-PCR. Real-time PCR revealed the effect of miR-124 overexpression on modulating gene expression changes in Huh7 and HepG2 cells. miR-124 transfection decreased expression of TNF by 87–88 % in both cell lines, with a 0.13-fold change in HepG2 ($p = 0.04$) and 0.12-fold change in Huh7 ($p = 0.03$). miR-124 also significantly reduced TLR4 expression in HepG2 cells by 88 % (0.12-fold, $p = 0.006$). Expression of SREBF2 was decreased by 87 % (0.127-fold, $p = 0.002$) following miR-124 transfection in HepG2 cells. Additionally, FASN expression was downregulated by 37 % (0.37-fold change, $P = 0.04$) in HepG2 cells and 91 % (0.09-fold change, $P = 0.03$) in Huh7 cells

Table 3 (*continued*)

2D structure of miR16 and miR124 interaction with gene targets	miRNA and gene interaction	mfe (kcal/mol)
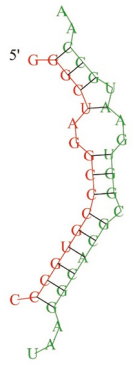	has-miR-124-3p: FASN	−25.9
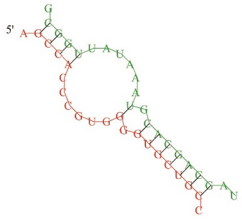	has-miR-16-5p: FASN	−25

Mfe: minimal free energy

transfected with miR-124. miR-124 overexpression also resulted in an 80 % reduction of TGFβ-1 expression in Huh7 cells (0.2-fold, $p = 0.018$) and 24 % reduction (0.24-fold change, $P = 0.048$) in HepG2 cells. SCD expression was lowered by 53 % (0.47-fold, $p = 0.008$) specifically in miR-124 transfected Huh7 cells (Fig. 3-B, C).

3.4.2. *Influence of miR-16 transfection on the target genes*

Real-time PCR results showed the effect of miR-16 overexpression on modulating target gene expression. SCD expression was decreased by 33 % (0.67-fold change) in HepG2 cells and 72 % (0.28-fold change) in Huh7 cells, with *p*-values of 0.023 and 0.046 respectively. TLR4 expression was downregulated by 34 % (0.66-fold change) in HepG2 cells and 65 % (0.35-fold change) in Huh7 cells, with p-values of 0.029 and 0.046 respectively. FASN expression was reduced by 70 % (0.3-fold change) in HepG2 cells and 64 % (0.64-fold change) in Huh7 cells, with p-values of 0.006 and 0.049 respectively. SREBF2 expression was decreased by 80 % (0.2-fold change) in HepG2 cells and 76 % (0.24-fold change) in Huh7 cells, with p-values of 0.02 and 0.048 respectively. While there were trends towards decreased TGFβ-1 and TNF expression, these changes did not reach statistical significance in either cell line model (Fig. 3-D, E).

3.5. *MTT assay for the Effect of miR-16 and miR-124 on cell viability*

Cell toxicity of miR-124 and miR-16 after transfection at the 24 h, 48 h, and 72 h time points with or without 0.5 mM oleic acid treatment were evaluated in the HepG2 and Huh7 cells. Cell viability was determined by comparison of treated groups to the empty vector group (Fig. 4A, B). There was a decrease in cell viability in both cell lines after 72 h with no difference at 24 h or 48 h (Except for miR-124 + oleic acid treatment in Huh7 cells after 48 h). In HepG2 cells at 72 h, miR-124 demonstrated a 24.7 % reduction in viability compared to empty vector (Mean Diff ± SE = 24.7 ± 1.45, $p = 0.009$). miR-16 decreased viability by 33 % (Mean Diff ± SE = 33 ± 3.05, $p = 0.022$). The combination of miR-124 and oleic acid reduced viability by 41.3 % (Mean Diff ± SE = 41.3 ± 4.7, $p = 0.033$), while miR-16 and oleic acid decreased viability by 27.7 % (Mean Diff ± SE = 27.7 ± 3, p = 0.03). In Huh7 cells at 72 h, viability was reduced by 29.33 % for miR-124 (Mean Diff ± SE = 29.33 ± 4.702, $p = 0.064$) and 32.3 % for miR-16 (Mean Diff ± SE = 32.3 ± 2.03, $p = 0.01$) compared to empty vector. miR-124 combined with oleic acid decreased Huh7 viability by 31.33 % (Mean Diff ± SE = 31.33 ± 1.2, $p = 0.004$), while miR-16 and oleic acid reduced viability by 33.0 % (Mean Diff ± SE = 33.00 ± 3.05, p = 0.02). However, in Huh7 cells, the results also indicate miR-124 might have cytotoxicity at 48 h after transfection ($P = 0.04$), with Mean Diff ± SE of diff = 42 ± 5.69. The results revealed that after 48 h of treatment, Huh7 cells exhibited increased sensitivity to miR-124 + oleic acid.

4. PAB test

The PAB test is performed by performing two enzymatic and chemical reactions. In the enzymatic reaction, tetramethylbenzidine chromogen is oxidized to cationic tetramethylbenzidine by hydrogen peroxide (oxidant) and, in the chemical reaction, cationic tetramethylbenzidine is reduced by uric acid (antioxidant).[40] In the one-way ANOVA test and Tukey's multiple comparisons test, no significant differences were observed among empty vector-oleic acid and miR-16 or miR-124 for alteration in oxidant/antioxidant balance based on the PAB test in either HepG2 and Huh7 cell lines (Fig. 5-A,B).

5. Discussion

NAFLD is a prevalent metabolic disorder that encompasses the spectrum from steatosis to steatohepatitis and hepatic fibrosis.[41] This condition is well acknowledged as a multi-factorial disorder involving interactions between susceptibility genes and risk factors that have a major role in the onset and progression of NAFLD.[42]

Recent pharmacology strategies are directed towards regulating several molecular targets in a multifaceted manner to enhance disease control.[17] By focusing on several critical genes and pathways implicated in the pathophysiology of illnesses like NAFLD, this strategy offers a platform to improve treatment efficacy.[12] Since miRNA-based medications have the capacity to modulate the expression of many genes implicated in a disease, they have potential as potent and effective therapeutic tools.[11,43,44] Although their interactions with mRNA are not well defined, miRNAs also have the ability to influence unintended pathways.[45]

Based on our previous *in silico* investigations, we predicted that miR-124 and miR-16 had the potential to target several key genes involved in NAFLD pathogenesis. Specifically, bioinformatics analysis identified these microRNAs as promising regulatory candidates targeting genes integral to lipogenesis, inflammation, and oxidative stress responses in the liver.[22] The current study aimed to validate these computational predictions experimentally using *in vitro* NAFLD cell culture models. The results demonstrated that overexpression of miR-124 and miR-16 directly decreased expression of several genes previously identified as putative targets. This occurred through significant downregulation at the mRNA level in both HepG2 and Huh7 hepatocyte cell lines subjected to lipotoxic conditions. Additionally, miR-124 and miR-16 modulated lipid accumulation and mediated cytotoxic effects in a time-dependent manner. Most notably, the microRNAs attenuated oleic acid-induced intracellular lipid droplet formation and reduced cell viability at later time points.

We show that miR-124 downregulates the expression of TNF, TLR4, FASN, SREBF2 and TGFβ-1 using real-time PCR in cells treated with 0.5 mM oleic acid. Moreover, miR-16 showed high suppression potential for genes involved in the progression of NAFLD, including TLR4, SCD, FASN and SREBF2. Furthermore, a concordance between minimal free energy on *in silico* prediction and the experimental level of suppression was observed. For instance, the MFE prediction of binding miR-124 and miR-16 to TGFB1 were −27.3 and 019.3, respectively, and real-time PCR indicated that miR-124 could significantly downregulate the expression of TGFB1 while miR-16 did not have an effect on expression of this gene.

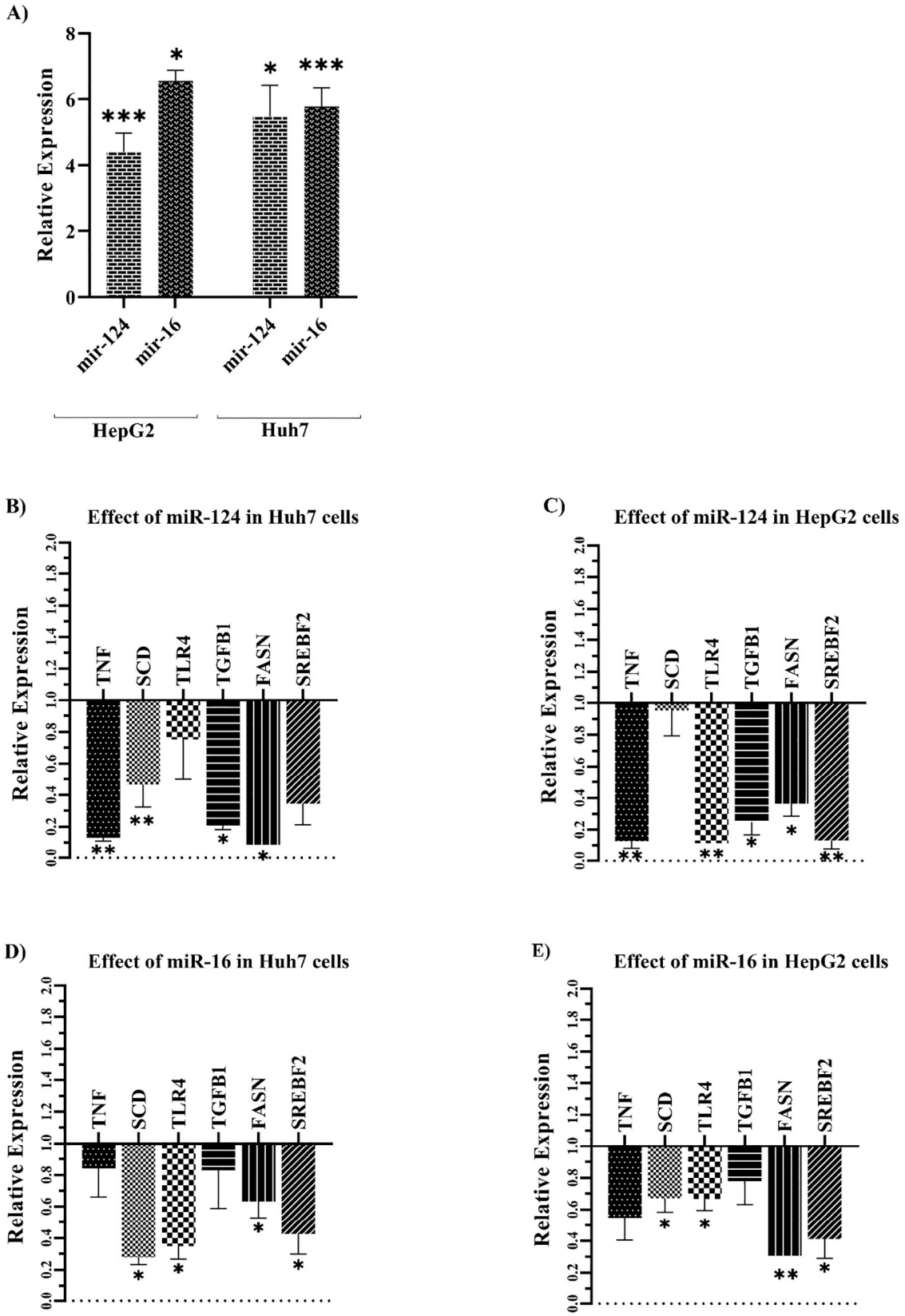

Fig. 3. Effect of miR-124 and miR-16 overexpression on the mRNA expression of genes implicated in NAFLD pathogenesis. Huh7 and HepG2 cells were cultured in 24-well plates and transfected with pLenti-III-16-GFP, pLenti-III-124-GFP or empty vector for 36 h using PolyFect Transfection Reagent. This was followed by 12 h of 0.5 mM oleic acid treatment to induce steatosis. (A) Real-time PCR validation showing significant overexpression of miR-124 and miR-16 after transfection compared to empty vector control. (B,C) Impact of miR-124 overexpression on the mRNA expression of TNF, SCD, TLR4, FASN, TGFβ-1, and SREBF2 in Huh7 (B) and HepG2 (C) cells. (D,E) Effect of miR-16 overexpression on the mRNA expression of SCD, TLR4, FASN, and SREBF2 in Huh7 (D) and HepG2 (E) cells. Data are shown as mean ± SEM. Statistical significance reported as $^{*}P < 0.05$ and $^{**}P < 0.01$, $^{***}P < 0.001$.

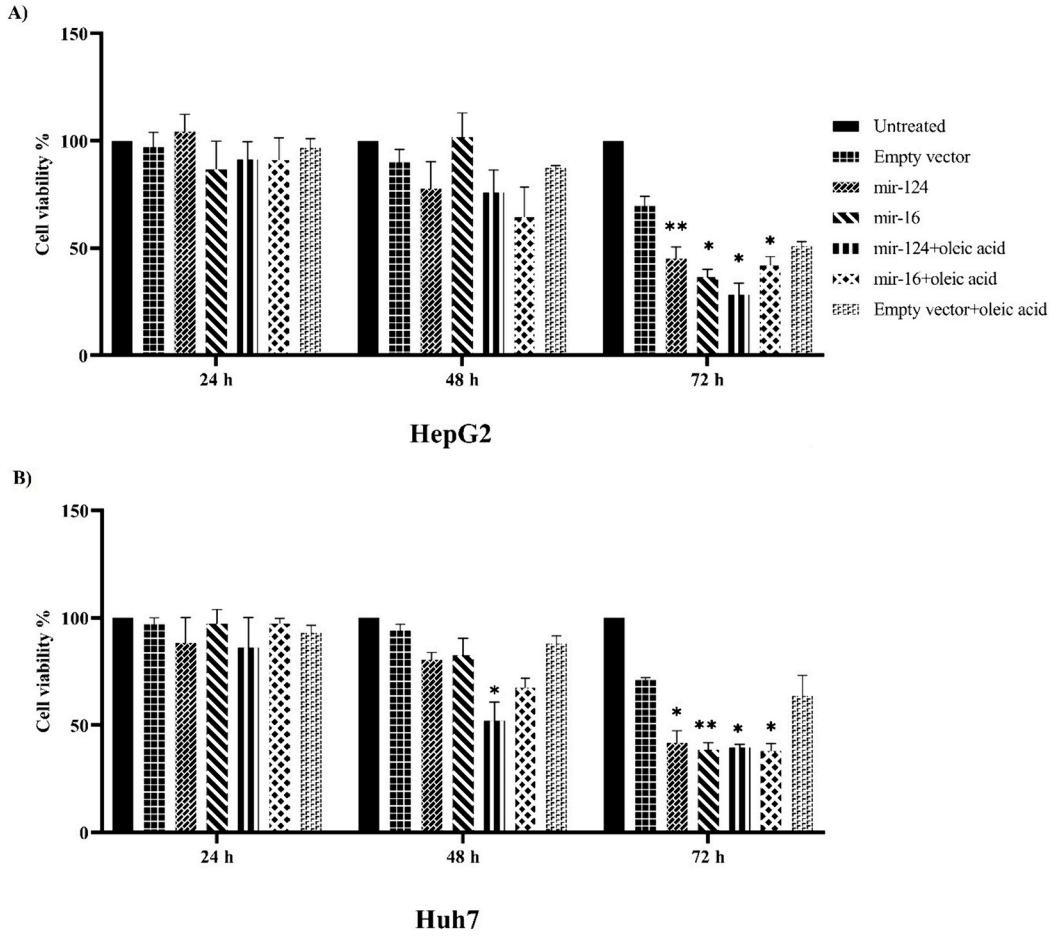

Fig. 4. Effect of miR-124 and miR-16 overexpression on cell viability over time assessed by MTT assay. Huh7 and HepG2 cells were seeded in 96-well plates and transfected with pLenti-III-16-GFP, pLenti-III-124-GFP or empty vector. After 0.5 mM oleic acid treatment, cell viability was measured at 24, 48, and 72 h post-transfection using the MTT assay. (A) In HepG2 cells, miR-124 and miR-16 overexpression significantly decreased viability by 24.7 % and 33 % respectively compared to empty vector control at 72 h. (B) In Huh7 cells, miR-124 overexpression significantly decreased viability by 42 % at 48 h and 29.33 % at 72 h compared to control. miR-16 overexpression also significantly decreased viability by 32.3 % at 72 h. No significant changes were observed at 24 h in either cell line. (*$P < 0.05$ and **$P < 0.01$).

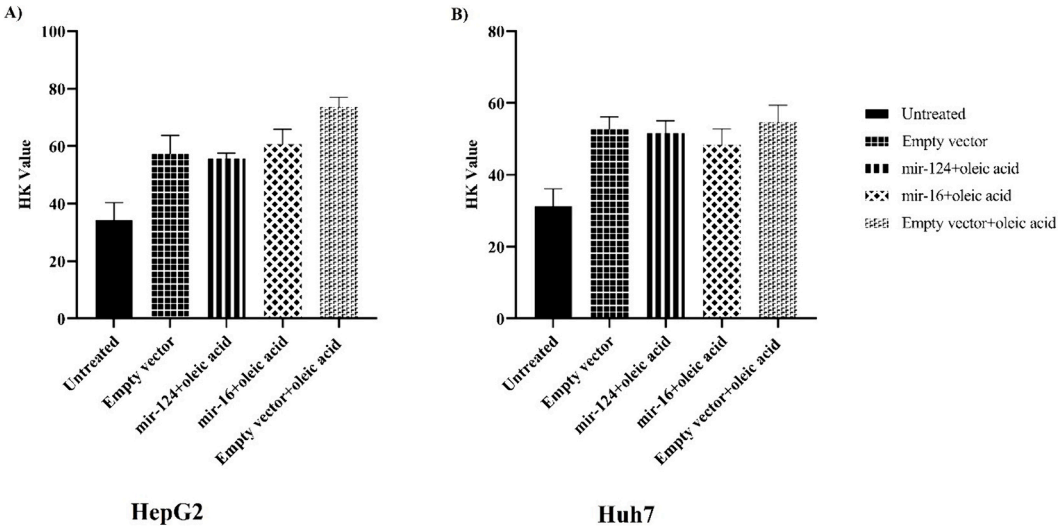

Fig. 5. Effect of miR-124 and miR-16 overexpression on pro-oxidant/antioxidant balance assessed by PAB assay. HepG2 and Huh7 cells were transfected with pLenti-III-16-GFP, pLenti-III-124-GFP or empty vector for 36 h, followed by 12 h of 0.5 mM oleic acid treatment. The PAB assay was then performed to simultaneously measure the total oxidant and antioxidant levels in cell lysates. (A) In HepG2 cells, no significant differences were observed in PAB values between empty vector, miR-124 or miR-16 transfected groups with or without oleic acid treatment, as analyzed by one-way ANOVA. (B) Similarly, in Huh7 cells no statistically significant changes in PAB were detected among the experimental groups.

MiR-124 is highly expressed in the brain and has also been identified in diverse tissues,[46] and published research reports its role in biological function in several diseases. MiR-124-3p functions in regulating autophagy through Beclin and LC3 in the liver[47] and it is also involved in the regulation of lipid homeostasis in liver metabolism in NAFLD.[33] It has been reported that miR-124 might diminish inflammation by modulating IL-4Rα signaling.[48] A recent report indicates that miR-124, by targeting G3BP Stress Granule Assembly Factor 2 (G3BP2) and triggering p38MAPK signaling, could alleviate dysfunction in high glucose-stimulated endothelial cells.[49] MiR-124 also plays a role in the inhibition of neuronal inflammation after traumatic brain injury.[50] In a recent study, miR-124 was shown to have a vital role in regulating pre-adipocyte adipogenesis[51] and atherosclerosis.[52] However, the function of miR-124 in metabolic diseases such as NAFLD is not yet well documented. In our study, we demonstrated that miR-124 had a significant impact on the *in vitro* NAFLD model created through oleic acid treatment. We showed that miR-124 significantly reduced lipid accumulation in both hepatic cell lines following treatment with oleic acid.

Several studies have demonstrated that overexpression of miR-124 has the potential to suppress the TLR4 signaling pathway.[29–31] One study indicated that miR-124, by downregulation of TLR4/MyD88/NF-κB p65 signaling, prevents the microglial proinflammatory response in palmitic acid-treated BV2 cells.[31] Another study reported that exosomal-miR-124 could decrease the level of TLR4 expression after traumatic brain injury.[29] In line with our data, the expression of TLR4 in HepG2 was significantly decreased following overexpression of miR-124 *via* transfection.

Another study found that transfection with a miR-124 mimic in bone marrow-derived macrophages could hinder osteoclastogenesis *via* regulating TNF-α.[53] An investigation by Zhang et al. in 2019 revealed that the level of TNF-α protein expression in a chronic sciatic nerve injury (CCI) rat model after treatment with miR-124-3p mimics was markedly decreased.[54] Using real-time PCR, we also showed that the expression level of TNF in both HepG2 and Huh7 cells was significantly downregulated following miR-124 transfection.

A recent report in 2020 by Li et al. indicated that miR-124 could impact the synthesis of fatty acids by suppressing SCD1 in brown adipocytes.[55] Another study reported that miR-124 regulates the expression of some critical enzymes in the β-oxidation and triglyceride homeostasis pathway.[56] Our results also indicate that miR-124 significantly downregulates SCD1 and FASN.

MiR-124 can hinder the proliferation of hypertrophic scar fibroblasts by targeting TGF-β1.[57] MiR-124 possibly regulates TGF-β by suppressing Wnt/β-catenin signaling.[58] Accordingly, we showed that miR-124 could decrease the expression of TGF-β which confirms the previous studies.

An analysis of miRNA profiles in NAFLD patients in 2021 by Vulf et al. indicated that miR-16-5p, in both the steatosis and steatohepatitis stages, was decreased.[32] A previous study confirmed by qPCR that miR-16 was decreased in the liver in a NALFD mouse model.[59] Another report also demonstrated that miR-16 is associated with the severity of NAFLD.[60] This downregulation of miR-16 is potentially linked to a protective function of miR-16 in the pathogenesis of NALFD. According to oil red O read staining, transfection with miR-16 in both HepG2 and Huh-7 cells treated with oleic acid led to a decrease in lipid accumulation.

Previously reports indicate that upregulation of miR-16 led to a reduction in the activity of TNF-α, an anti-inflammatory effect.[61,62] Although our results could not statistically confirm this, there was a trend towards a decrease in TNF expression after miR16 transfection into the HepG2 and Huh7 cell lines.

In several previous publications, the anti-fibrotic effect of mi-16, through suppressing the TGFβ-1 signaling pathway, was documented.[63–65] MiR-16, *via* regulation of the Smad2/3 pathway, exerted its anti-fibrotic activity.[63] In our results, however, the expression of TGFβ-1 showed a trend towards a decrease but this did not reach statistical significance. There are several potential factors that could explain why our results did not demonstrate a statistically significant effect of miR-16 on TNF and TGFβ-1 expression, despite previous reports indicating regulatory roles. Firstly, differences in cell types, disease models and experimental conditions between studies may influence a miRNA's activity and target regulation. Our study used liver cell lines under an oleic acid-induced NAFLD model, whereas previous works investigated other tissue/disease contexts. Additionally, the 48-h treatment duration in our study may not have been sufficient time for miR-16 to exert measurable effects on these genes. While the MTT and cytotoxicity assays limited extending treatment, longer durations could have allowed more prominent regulation to manifest and possibly achieve statistical significance. It is also possible that miR-16 does modulate TNF and TGFβ-1, but to a degree below our assays' level of detection. Larger sample sizes might help validate trends as statistically significant given inherent biological variability between experiments.

MiR-16 also markedly contributes to repressing FASN expression *via* a seed containing eight repeats of the FASN 3′-UTR region.[66] Our results indicate that transfection of miR-16 significantly downregulated the level of FASN in both liver cancer cell lines following treatment with oleic acid.

Another report showed that miR-16 could directly affect TLR4. Using transfection with miR-16 mimics, *via* targeting TLR4, reduced the levels of the NLRP3 inflammasome, NF-κB and inflammatory factors.[67] Another recent study confirmed the inhibition of TLR4 due to overexpression of miR-16.[28] In line with our results, overexpression of miR-16 significantly decreased the expression of TLR4.

Based on the MTT assay, miR-124 and miR-16 at 72 h showed cytotoxicity which likely relates to the anticancer effects of these miRNAs.[68,69] Moreover, miR-124 at 46 h showed cytotoxicity in the Huh7 cell line. To overcome this issue, one potential approach is to use lower doses of a combination of several miRNAs that synergistically modulate the expression of the same gene targets.[70] However, miRNA delivery to the target site, such as the liver, could minimize their toxicity and any adverse effects as well as increase the therapeutic effect, as previously indicated.[71]

The aggregate production of reactive oxygen species (ROS) which leads to oxidative stress contributes to the pathogenesis of chronic and acute liver disorders especially NAFLD. NAFLD is a redox-centered disorder due to the function of ROS in hepatic metabolism.[72] The results from the anti-oxidant and oxidant tests were consistent with previous studies reporting significantly decreased antioxidant activity in liver cancer cell lines treated with oleic acid.[73–75] However, the non-significant increase observed in the PAB test as an indicator of higher oxidant component does not necessarily negate previous findings. Individual studies have demonstrated that miR-124-3p overexpression decreased malondialdehyde (MDA) levels and increased superoxide dismutase (SOD) and plasma glutathione peroxidase (GSH-Px) levels in keratinocytes,[76] while miR-16-5p was reported to promote ER stress and oxidative stress in cardiac cells.[77] However, our study did not directly measure other markers of oxidative stress such as SOD, Catalase (CAT) and MDA levels, which could have provided additional insights into how these miRNAs modulate oxidative status under oleic acid-induced NAFLD conditions. It is possible they exert antioxidant effects through alternative mechanisms not detected by the PAB assay alone. Previous reports also investigated different disease models and cell types compared to our study. Cell- and disease-specific factors may influence a miRNA's role. A more comprehensive assessment of oxidative stress indicators is warranted, such as quantifying antioxidant enzyme activities and lipid peroxidation.

It is important to acknowledge several limitations associated with the study design. Firstly, the use of *in vitro* cell culture models does not fully replicate the complexity of the *in vivo* liver microenvironment, which consists of diverse interacting cell types. While transient transfection *via* PolyFect allowed for investigation of mRNA effects, longer-term analysis of miRNA expression using viral vectors would be necessary to understand temporal dynamics, which was not feasible with the

single time point examined. Moreover, the study focused solely on changes at the transcriptional level and did not assess functional protein or post-transcriptional impacts, which may not necessarily correlate. Furthermore, the study utilized a single-cell model induced by oleic acid, representing only one etiological stage of NAFLD, while it is crucial to explore multiple disease triggers and progressive stages. Addressing these interconnected limitations through optimized methodologies that incorporate *in vivo* validation, kinetic profiling, expanded target assessment, and additional disease modeling would significantly strengthen future investigations into the therapeutic potential of miRNAs.

6. Conclusion

In summary, this studied showed the impact of miR-16 and miR-124 on suppression of the expression of critical genes involved in NAFLD and, as a result, alleviated the NAFLD disorder in an *in vitro* model induced by oleic acid. Notably, miR-16 and miR-124 displayed partial cytotoxicity at 72 h which is possibly related to their anti-cancer properties. Our results were unable to confirm the antioxidant activity of miR-16 and miR-124. However, further *in vivo* investigations are required to evaluate both the therapeutic and side effects of miR-16 and miR-124. Future research may clarify the suppression effects of miR-16 and miR-124 on protein levels as well as their ability to modulate the progression of different stages of NAFLD.

CRediT authorship contribution statement

Ali Mahmoudi: Conceptualization, Formal analysis, Investigation, Methodology, Writing – original draft. **Amin Jalili:** Conceptualization, Funding acquisition, Investigation, Methodology, Resources, Supervision, Writing – review & editing. **Seyed Hamid Aghaee-Bakhtiari:** Investigation, Writing – review & editing. **Reza Kazemi Oskuee:** Investigation, Writing – review & editing. **Alexandra E. Butler:** Investigation, Writing – review & editing. **Manfredi Rizzo:** Investigation, Writing – review & editing. **Amirhossein Sahebkar:** Conceptualization, Investigation, Methodology, Resources, Writing – review & editing.

Declaration of competing interest

The authors have no conflict of interests to declare.

Acknowledgment

This study was financially supported by the Mashhad University of Medical Sciences (grant code 990706). This paper is part of the PhD thesis of the first author.

References

1.. Liu D, et al. Ets-1 deficiency alleviates nonalcoholic steatohepatitis via weakening TGF-β1 signaling-mediated hepatocyte apoptosis. *Cell Death Dis*. 2019;10:458.
2. Bessone F, Razori MV, Roma MG. Molecular pathways of nonalcoholic fatty liver disease development and progression. *Cell Mol Life Sci*. 2019;76:99–128.
3. Mittal S, et al. Hepatocellular carcinoma in the absence of cirrhosis in United States veterans is associated with nonalcoholic fatty liver disease. *Clin Gastroenterol Hepatol*. 2016;14:124–131 [e1].
4. Dyson J, et al. Hepatocellular cancer: the impact of obesity, type 2 diabetes and a multidisciplinary team. *J Hepatol*. 2014;60:110–117.
5. Piscaglia F, et al. Clinical patterns of hepatocellular carcinoma in nonalcoholic fatty liver disease: a multicenter prospective study. *Hepatology*. 2016;63:827–838.
6. Magee N, Zou A, Zhang Y. Pathogenesis of nonalcoholic Steatohepatitis: interactions between liver parenchymal and nonparenchymal cells. *Biomed Res Int*. 2016;2016, 5170402.
7. Ludwig J, et al. Nonalcoholic steatohepatitis: Mayo Clinic experiences with a hitherto unnamed disease. *Mayo Clin Proc*. 1980;55:434–438.
8. Petta S, et al. Pathophysiology of non alcoholic fatty liver disease. *Int J Mol Sci*. 2016;17:2082.
9.. Nair B, Nath LR. Inevitable role of TGF-β1 in progression of nonalcoholic fatty liver disease. *J Recept Signal Transduction*. 2020;40:195–200.
10. Manne V, Handa P, Kowdley KV. Pathophysiology of nonalcoholic fatty liver disease/nonalcoholic Steatohepatitis. *Clin Liver Dis*. 2018;22:23–37.
11. Mahmoudi A, et al. Investigation of the effect of curcumin on protein targets in NAFLD using bioinformatic analysis. *Nutrients*. 2022;14:1331.
12. Mahmoudi A, et al. Target deconvolution of fenofibrate in nonalcoholic fatty liver disease using bioinformatics analysis. *Biomed Res Int*. 2021;2021, 3654660.
13. Mahmoudi A, et al. Impact of fenofibrate on NAFLD/NASH: a genetic perspective. *Drug Discov Today*. 2022;27:2363–2372.
14. Mahmoudi A, et al. The role of exosomal miRNA in nonalcoholic fatty liver disease. *J Cell Physiol*. 2022;237:2078–2094.
15. Sookoian S, Pirola CJ. Precision medicine in nonalcoholic fatty liver disease: new therapeutic insights from genetics and systems biology. *Clin Mol Hepatol*. 2020;26:461–475.
16.. Nobili V, Alisi A. *NAFLD in children: new genes, new diagnostic modalities and new drugs*. 16(9). 2019:517–530.
17. Bajan S, Hutvagner G. RNA-based therapeutics: from antisense oligonucleotides to miRNAs. *Cells*. 2020;9:137.
18. Mahjoubin-Tehran M, et al. Harnessing the therapeutic potential of decoys in non-atherosclerotic cardiovascular diseases: state of the art. *J Cardiovasc Dev Dis*. 2021;8:103.
19. Mahjoubin-Tehran M, et al. Decoy technology as a promising therapeutic tool for atherosclerosis. *Int J Mol Sci*. 2021;22:4420.
20. Mahmoudi A, et al. Liver protective effect of Fenofibrate in NASH/NAFLD animal models. *PPAR Res*. 2022;2022, 5805398.
21. Mahmoudi A, et al. Effect of curcumin on attenuation of liver cirrhosis via genes/proteins and pathways: a system pharmacology study. *Nutrients*. 2022;14. https://doi.org/10.3390/nu14204344.
22. Mahmoudi A, et al. Exploration of the key genes involved in non-alcoholic fatty liver disease and possible microRNA therapeutic targets. *J Clin Exp Hepatol*. 2024.
23. Vahdat Lasemi F, et al. Harnessing nucleic acid-based therapeutics for atherosclerotic cardiovascular disease: state of the art. *Drug Discov Today*. 2019;24:1116–1131.
24.. Gjorgjieva M, et al. miRNAs and NAFLD: from pathophysiology to therapy. *Gut*. 2019;68:2065–2079.
25. Lam JKW, et al. siRNA versus miRNA as therapeutics for gene silencing. *Mol Ther Nucleic Acids*. 2015;4, e252.
26. Ardekani AM, Naeini MM. The role of MicroRNAs in human diseases. *Avicenna J Med Biotechnol*. 2010;2:161–179.
27.. Wang X, et al. MicroRNAs as regulators, biomarkers and therapeutic targets in liver diseases. *Gut*. 2021;70:784–795.
28.. Xi M, et al. MicroRNA-16 inhibits the TLR4/NF-κB pathway and maintains tight junction integrity in irritable bowel syndrome with diarrhea. *J Biol Chem*. 2022;298, 102461.
29. Yang Y, et al. MiR-124 enriched exosomes promoted the M2 polarization of microglia and enhanced hippocampus neurogenesis after traumatic brain injury by inhibiting TLR4 pathway. *Neurochem Res*. 2019;44:811–828.
30.. Li QR, et al. MicroRNA-124 alleviates hyperoxia-induced inflammatory response in pulmonary epithelial cell by inhibiting TLR4/NF-κB/CCL2. *Int J Clin Exp Pathol*. 2018;11:76–87.
31. Yang C, et al. MiR-124 prevents the microglial proinflammatory response by inhibiting the activities of TLR4 and downstream NLRP3 in palmitic acid-treated BV2 cells. *J Mol Neurosci*. 2022;72:496–506.
32. Vulf M, et al. Analysis of miRNAs profiles in serum of patients with steatosis and Steatohepatitis. *Front Cell Dev Biol*. 2021;9, 736677.
33. Wang G, et al. Repression of MicroRNA-124-3p alleviates high-fat diet-induced Hepatosteatosis by targeting Pref-1. *Front Endocrinol (Lausanne)*. 2020;11, 589994.
34. Krüger J, Rehmsmeier M. RNAhybrid: microRNA target prediction easy, fast and flexible. *Nucleic Acids Res*. 2006;34:W451–W454.
35. Jafari Najaf Abadi MH, et al. miR-27 and miR-124 target AR coregulators in prostate cancer: bioinformatics and in vitro analysis. *Andrologia*. 2022.
36.. Aghaee-Bakhtiari SH, et al. MAPK and JAK/STAT pathways targeted by miR-23a and miR-23b in prostate cancer: computational and in vitro approaches. *Tumor Biol*. 2015;36:4203–4212.
37. Livak KJ, Schmittgen TD. Analysis of relative gene expression data using real-time quantitative PCR and the 2(-Delta Delta C(T)) method. *Methods*. 2001;25:402–408.
38. Zahedi Avval F, et al. Determining pro-oxidant antioxidant balance (PAB) and Total antioxidant capacity (TAC) in patients with schizophrenia. *Iran J Psychiatry*. 2018;13:222–226.
39. Alamdari DH, et al. A novel assay for the evaluation of the prooxidant-antioxidant balance, before and after antioxidant vitamin administration in type II diabetes patients. *Clin Biochem*. 2007;40:248–254.
40. Ghazizadeh H, et al. Pro-oxidant–antioxidant balance (PAB) as a prognostic index in assessing the cardiovascular risk factors: a narrative review. *Obesity Med*. 2020;19, 100272.
41.. Sinton MC, Hay DC, Drake AJ. *Metabolic control of gene transcription in non-alcoholic fatty liver disease: the role of the epigenome*. 11(1). 2019:104.
42. Eslam M, Valenti L, Romeo S. Genetics and epigenetics of NAFLD and NASH: clinical impact. *J Hepatol*. 2018;68:268–279.
43. Giral H, Kratzer A, Landmesser U. MicroRNAs in lipid metabolism and atherosclerosis. *Best Pract Res Clin Endocrinol Metab*. 2016;30:665–676.
44. Niu N, et al. Targeting mechanosensitive transcription factors in atherosclerosis. *Trends Pharmacol Sci*. 2019;40:253–266.
45. Gumienny R, Zavolan M. Accurate transcriptome-wide prediction of microRNA targets and small interfering RNA off-targets with MIRZA-G. *Nucleic Acids Res*. 2015;43:1380–1391.

46. Ghafouri-Fard S, et al. An update on the role of miR-124 in the pathogenesis of human disorders. *Biomed Pharmacother*. 2021;135, 111198.
47.. Niu Y, et al. miR-124-3p and miR-140-3p. 2 act as negative regulators of Beclin1 and LC3 expression in the liver of rat model with hepatic impact injury. *Bio Res*. 2018:29.
48.. Liu Q, et al. Increased miR-124-3p alleviates type 2 inflammatory response in allergic rhinitis via IL-4Rα. *Inflamm Res*. 2022;71:1271–1282.
49. Zhao H, He Y. MiR-124-3p suppresses the dysfunction of high glucose-stimulated endothelial cells by targeting G3BP2. *Front Genet*. 2021;12, 723625.
50. Huang S, et al. Increased miR-124-3p in microglial exosomes following traumatic brain injury inhibits neuronal inflammation and contributes to neurite outgrowth via their transfer into neurons. *FASEB J*. 2018;32:512–528.
51. Lin W, et al. SESN3 inhibited SMAD3 to relieve its suppression for MiR-124, thus regulating pre-adipocyte Adipogenesis. *Genes (Basel)*. 2021;12.
52. Mahjoubin-Tehran M, et al. In silico and in vitro analysis of microRNAs with therapeutic potential in atherosclerosis. *Sci Rep*. 2022;12:1–16.
53.. Ohnuma K, et al. MicroRNA-124 inhibits TNF-α- and IL-6-induced osteoclastogenesis. *Rheumatol Int*. 2019;39:689–695.
54.. Zhang Y, et al. miR-124-3p attenuates neuropathic pain induced by chronic sciatic nerve injury in rats via targeting EZH2. *J Cell Biochem*. 2019;120:5747–5755.
55. Li Q, et al. Roles of miR-124-3p/Scd1 in urolithin A-induced brown adipocyte differentiation and succinate-dependent regulation of mitochondrial complex II. *Biochem Biophys Res Commun*. 2022;606:174–181.
56. Shaw TA, et al. MicroRNA-124 regulates fatty acid and triglyceride homeostasis. *iScience*. 2018;10:149–157.
57.. Zhang S, Pan S. miR-124-3p targeting of TGF-β1 inhibits the proliferation of hypertrophic scar fibroblasts. *Adv Clin Exp Med*. 2021;30:263–271.
58.. Lu Y, et al. MiR-124 regulates transforming growth factor-β1 induced differentiation of lung resident mesenchymal stem cells to myofibroblast by repressing Wnt/β-catenin signaling. *Dev Biol*. 2019;449:115–121.
59. Kim JH, et al. Reverse expression of aging-associated molecules through transfection of miRNAs to aged mice. *Mol Ther Nucleic Acids*. 2017;6:106–115.
60.. López-Riera M, et al. *Non-invasive prediction of NAFLD severity: a comprehensive, independent validation of previously postulated serum microRNA biomarkers*. 8(1). 2018 [10606].
61. Zhang K, et al. Upregulated gga-miR-16-5p inhibits the proliferation cycle and promotes the apoptosis of MG-infected DF-1 cells by repressing PIK3R1-mediated the PI3K/Akt/NF-κB pathway to exert anti-inflammatory effect. *Int J Mol Sci*. 2019;20.
62.. Yamada K, et al. MicroRNA 16-5p is upregulated in calorie-restricted mice and modulates inflammatory cytokines of macrophages. *Gene*. 2020;725, 144191.
63.. Ma L, et al. MiR-15b and miR-16 suppress TGF-β1-induced proliferation and fibrogenesis by regulating LOXL1 in hepatic stellate cells. *Life Sci*. 2021;270, 119144.
64.. Jin W, et al. miR-15a/miR-16 cluster inhibits invasion of prostate cancer cells by suppressing TGF-β signaling pathway. *Biomed Pharmacother*. 2018;104:637–644.
65.. Wang H, et al. miR-16 mimics inhibit TGF-β1-induced epithelial-to-mesenchymal transition via activation of autophagy in non-small cell lung carcinoma cells. *Oncol Rep*. 2018;39:247–254.
66.. Wang J, et al. Fatty acid synthase is a primary target of MiR-15a and MiR-16-1 in breast cancer. *Oncotarget*. 2016;7:78566–78576.
67.. Yang Y, et al. miR-16 inhibits NLRP3 inflammasome activation by directly targeting TLR4 in acute lung injury. *Biomed Pharmacother*. 2019;112, 108664.
68.. Xu Y, et al. Anticancer effects of miR-124 delivered by BM-MSC derived exosomes on cell proliferation, epithelial mesenchymal transition, and chemotherapy sensitivity of pancreatic cancer cells. *Aging*. 2020;12:19660–19676.
69. Ghafouri-Fard S, et al. A review on the role of mir-16-5p in the carcinogenesis. *Cancer Cell Int*. 2022;22:342.
70. Segal M, Slack FJ. Challenges identifying efficacious miRNA therapeutics for cancer. *Expert Opin Drug Discovery*. 2020;15:987–991.
71. Zhang S, et al. The risks of miRNA therapeutics: in a drug target perspective. *Drug Des Devel Ther*. 2021;15:721.
72. Hong T, et al. The role and mechanism of oxidative stress and nuclear receptors in the development of NAFLD. *Oxid Med Cell Longev*. 2021;2021, 6889533.
73.. Zhang J, et al. Pinolenic acid ameliorates oleic acid-induced lipogenesis and oxidative stress via AMPK/SIRT1 signaling pathway in HepG2 cells. *Eur J Pharmacol*. 2019;861, 172618.
74.. He Y, et al. Silencing HIF-1α aggravates non-alcoholic fatty liver disease in vitro through inhibiting PPAR-α/ANGPTL4 singling pathway. *Gastroenterol Hepatol*. 2021;44:355–365.
75. Huang B, et al. Cytochrome P450 1A1 (CYP1A1) catalyzes lipid peroxidation of oleic acid-induced HepG2 cells. *Biochemistry (Mosc)*. 2018;83:595–602.
76. Liu S, Gong J. miR-124-3p delivered using exosomes attenuates the keratinocyte response to IL-17A stimulation in psoriasis. *Oxid Med Cell Longev*. 2022;2022, 6264474.
77. Toro R, et al. miR-16-5p suppression protects human cardiomyocytes against endoplasmic reticulum and oxidative stress-induced injury. *Int J Mol Sci*. 2022;23.